ORIGINAL ARTICLE

Immunology WILEY

Galectin-3 interacts with PD-1 and counteracts the PD-1 pathway-driven regulation of T cell and osteoclast activity in Rheumatoid Arthritis

Kathrine Pedersen[1] | Morten Aagaard Nielsen[1,2] | Kristian Juul-Madsen[1,3] | Malene Hvid[1,4] | Bent Deleuran[1,2] | Stinne Ravn Greisen[1,2]

[1]Department of Biomedicine, Aarhus University, Aarhus, Denmark

[2]Department of Rheumatology, Aarhus University Hospital, Aarhus, Denmark

[3]Max-Delbrück-Center for Molecular Medicine, Berlin, Germany

[4]Department of Clinical Medicine, Aarhus University, Aarhus, Denmark

Correspondence
Stinne Ravn Greisen, Høegh-Guldbergs Gade 10 DK-8000 Aarhus C Denmark.
Email: srg@biomed.au.dk

Funding information
Aase og Ejnar Danielsens Fond, Grant/Award Number: 20-10-0363

Abstract

Rheumatoid arthritis (RA) is an autoimmune disease characterized by joint inflammation and bone erosions. The glycosylated programmed death-1 (PD-1) receptor plays an important role in regulating immune responses and maintaining tolerance. In this study, we focus on two features observed in RA: impaired PD-1 signalling and Galectin-3 (Gal-3) upregulation. We hypothesize that Gal-3 binds PD-1 and PD-1 ligands, potentially contributing to impaired PD-1 signalling. PD-1 and Gal-3 levels in RA synovial fluid (SF) and plasma were evaluated by ELISA. PD-1 and Gal-3 interaction was examined by Surface Plasmon Resonance and ELISA. PD-1, PD-L1 and Gal-3 expression on mononuclear cells from SF and peripheral blood as well as fibroblast-like synoviocytes were examined by flow cytometry. Effects of Gal-3 and PD-L1 on osteoclast formation was evaluated by tartrate-resistant acid phosphatase assay. We show that Gal-3 binds PD-1 and PD-L1. Results demonstrated high expression of PD-1 and Gal-3 on mononuclear cells, especially from SF. Gal-3 inhibited PD-1 signalling when PD-L1 was present. Furthermore, a role of Gal-3 in osteoclast formation was observed in vitro, both directly but also through PD-1:PD-L1 inhibition. Effects of Gal-3 on the PD-1 signalling axis are proposed to be inhibitory, meaning high Gal-3 levels in the complex synovial microenvironment are not desirable in RA. Preventing Gal-3′s inhibitory role on PD-1 signalling could, therefore, be a therapeutic target in RA by affecting inflammatory T cell responses and osteoclasts.

1 | INTRODUCTION

Rheumatoid arthritis (RA) is a chronic autoimmune disease affecting the joints.[1,2] Despite targeted treatment, inflammation is inadequately controlled in 30% of RA patients, resulting in joint destruction. In the synovium various cell types are central in driving inflammation, among these are T cells and synovial fibroblasts. T cells produce pro-inflammatory cytokines.[3,4] Cytokines also activate synovial fibroblasts, which subsequently contribute to the

inflammation and bone destruction by producing matrix metalloproteinases and inducing the expression of receptor activator of nuclear factor kappa-B ligand (RANKL).[5,6] T cells are thus a central driver of inflammation in RA.

Under normal conditions, T cell activity will decrease when the pathological agent is no longer present. This downregulation is maintained by immune checkpoint inhibitors to prevent autoimmunity.[7] Programmed Death 1 (PD-1) is a glycosylated inhibitory immune checkpoint receptor present on both activated CD4+ and CD8+ T cells.[7–9] This receptor plays an important role in regulating the immune response and maintaining tolerance.[7] When PD-1 is engaged by its ligands, PD-L1 or PD-L2, the downstream signalling pathway causes downregulation of T cell receptor signalling and hereby inhibits T cell effector functions. This results in a decrease in cytokine production, proliferation and cytolytic function.[10]

In cancer, tumour cells induce expression of PD-L1 and signal through the PD-1 pathway to escape immune surveillance,[11] and PD-1/PD-L1 blockade is considered a breakthrough in cancer treatment, even though some patients experience immune related adverse events (irAE) following treatment.[12] In contrast to cancer, PD-1 signalling is considered to be desirable in autoimmune diseases, like RA[13] and targeting the PD-1 pathway through PD-L1 ameliorates disease activity in a collagen-induced arthritis mouse model.[13] The presence of membrane-bound PD-1 is also associated with a milder course of disease.[14] However, results indicate that PD-1 signalling is downregulated during disease progression.[14] This suggests that PD-1 pathway stimulation is a potential novel treatment for RA patients comparable to a Cytotoxic T-lymphocyte-associated protein 4 (CTLA4) analogue, which bind the costimulatory molecules CD80/86 on antigen-presenting cells and thereby inhibits the interaction with CD28 on T cells. The CTLA4 analogue is already implemented in the clinic.[15] Additionally, we previously reported that the PD-1 pathway plays an important role in maintaining bone homeostasis.[16,17] In RA, CD4+ T cells are known to be key mediators of tissue damage,[18] supporting the close association between the PD-1 system and bone homeostasis.

In contrast, a subset of PD-1^{hi} T helper cells has been identified in seropositive RA and suggested to enable B cell help and thereby promote autoantibody production.[19] These findings highlight the complexity of the PD-1 system.

Immune checkpoint molecules can be regulated at multiple levels. In addition to transcriptional regulation, post-translational modifications such as glycosylation of PD-1 and PD-L1 regulates protein stability and interaction.[8] Furthermore, Galectin-9 (Gal-9) have recently been shown to bind to PD-1 and modulate the pathway[20] by binding to the putative n-linked glycosylation sites (N49, N58, N74 and N116) found on PD-1.

Galectin-3 (Gal-3) is a member of the galectin family of 15 animal lectins with well conserved carbohydrate-recognition domains (CRDs) for β-galactosides.[21] Gal-3 is the sole member of the chimera-type galectin and it is structurally unique among galectins, consisting of only one CRD linked to an N-terminal peptide domain.[22] Furthermore, Gal-3 stands out among galectins based on a strong association with the pathogenesis of RA, affecting the activity and inflammatory properties of osteoclasts, T cells and stromal cells.[23–25]

Gal-3 is elevated in plasma from both treatment-naïve patients and patients with long-standing RA.[26,27] In a CIA rat model, increased levels of Gal-3 were present in the synovium and Gal-3 levels correlated with disease progression.[28,29] These data correspond with RA patient synovium data, demonstrating increased Gal-3 expression and secretion.[26] The increase in Gal-3 levels has been shown to activate and induce secretion of pro-inflammatory cytokines from synovial fibroblasts.[26] In addition, Gal-3 is involved in cartilage degeneration by inducing Matrix Metalloproteinase 3 expression[30,31] and some studies also support the idea that Gal-3 is capable of inhibiting osteoblast differentiation as well as promoting osteoclastogenesis, resulting in bone destruction.[27,28,32,33]

Since PD-1 and PD-L1 are post-translationally modified by glycosylation and known to express n-linked glycosylation sites predicted to bind Galectins, we investigated if Gal-3 binds PD-1 or PD-L1 and influence signalling through the PD-1 pathway.

2 | METHODS

2.1 | Patients and healthy controls

RA patient samples from the Inflammation in Arthritis (INART) biobank were randomly chosen for this study. Patient material consisted of plasma, synovial fluid (SF) as well as fibroblast-like synoviocytes (FLS), and mononuclear cells from peripheral blood (PBMCs) and SF (SFMCs). All patients were chronic RA patients (n = 41, age: 52.3 ± 4.51, sex [female%]: 67.5%) and samples were collected when patients presented with disease flare. Healthy control (HC, n = 15, age: 40.5 ± 7.76, sex [female%]: 53.3%) samples were provided by the Danish blood bank.

2.2 | ELISA

Levels of sPD-1 and Gal-3 were measured by sandwich ELISA (PD-1: R&D systems, DY1086, Gal-3: R&D systems, DGAL30). Samples were run in duplicates. In the

PD-1 ELISA, bovine, goat and mouse IgG was added to the samples to block heterophilic antibodies against animal proteins.[34] Optical Density (OD) values were read in a microplate reader at 450 nm with a 570 nm reference.

A combinatorial ELISA setup was used to investigate Gal-3′s binding of sPD-1. In brief, wells were coated with rhGal-3 (1 μg/mL) (R&D systems, DGAL30). Detection was done with PD-1 detection antibody from the PD-1 ELISA kit (PD-1: R&D systems, DY1086). Samples included RA SF, RA plasma and HC plasma.

2.3 | Surface plasmon resonance

Surface Plasmon Resonance (SPR) was performed on the Biacore 3000 instrument (Biacore, Molecular Interactions Core Facility, AU). Binding was investigated between the recombinant human proteins; rhGal-3 (E.coli produced as described by Salomonsson et al.[35] kindly provided by Prof. Hakon Leffler), rhPD-1 (R&D systems, 1086-PD) and rhPD-L1 (R&D systems, 156-B7-100). PD-1 or PD-L1 was immobilized on the surface by protein G coupling. Increasing concentrations of rhGal-3 was injected in the flow cell. Lactose was used as control to inhibit Gal-3 binding.

The two-dimensional fits were made on the MATLAB 2012a platform (Mathworks) using the fitting tool EVILFIT version 3 software created by Peter Schuck as previously described.[36,37] In brief, input values matched the start and end injection time and included concentrations spanning from 62.5 nM to 500 nM for Gal-3 to PD-1 and from 15.6 nM to 4000 nM for Gal-3 to PD-L1. The association phase was fitted from t = 'injection start' plus 1 s to t = 'injection end' minus 5 s. Dissociation phase was fitted from t = 'injection end' plus 5 s to t = 'injection end' plus 200–300 s. The operator-set boundaries for the distributions were uniformly set to limit K_D values in the interval from 10^{-9} to 10^{-2} M, and k_{off} values in the interval from 10^{-5} to 10^1 s − 1 to ensure comparable and best quality fits reflected in a high signal to rmsd ratio. The distribution P (k_a, K_A) is calculated using the discretization of the equation:

$$R_{total} = \int_{K_A min}^{K_A max} \int_{k_a min}^{k_a max} R(k_a, K_A, C_{analyte}) P(k_a, K_A) dk_a \, dK_A$$

in a logarithmic grid of ($k_{a,i}$, $K_{A, i}$) values with 21 and 18 grid points distributed on each axis, respectively. This was done through a global fit to association and dissociation traces at the above-mentioned analyte concentrations. Tikhonov regularization was used as described by Zhao et al.[38] at a confidence level of $P = .95$ to determine the most

parsimonious distribution that is consistent with the data, showing only features that are essential to fit the data.

2.4 | Cell stimulation assays

RA SFMCs, RA and HC PBMCs were stimulated for 24 h with anti-CD3 (1 μg/mL, Okt3, Peprotech, 05121-20-100) and anti-CD28 (0.5 μg/mL, BD, 555725) prior to flowcytometric assessment of PD-1 and Gal-3 expression.

To determine intracellular IL-2 levels, HC PBMCs were stimulated with phytohemagglutinin (PHA, 5 μg/mL, A10978) for 48 h, then rested overnight in serum free media. CD4+ cells were isolated by negative selection (EasySep™ Human CD4+ T Cell Isolation Kit, StemCell Technologies, 17952). CD4+ T cells were subsequently stimulated with anti-CD3/anti-CD28 and given either of the following treatment for 4 h: rhPD-1, rhPD-L1, rhGal-3, rhGal-3 + rhPD-1 or rhGal-3 + rhPD-L1 (all 1 μg/mL). Brefeldin A (BFA) (10 μg/mL, Sigma, B7651-5 mg) was added to inhibit intracellular protein transport.

Fibroblast-like synoviocytes (FLS) were cultured from RA SFMC as previously described.[39,40] FLS at passage 4–5 were cultured in a 6-well plate (30 000 cells/well). When confluent, cells were stimulated with Tumour Necrosis Factor (TNF)-α (10 ng/mL) or interferon (IFN)-γ (10 ng/mL) for 48 h and stained for flow cytometry. Additionally, FLS were used in a stimulation assay. FLS were seeded out in a 96-well plate (10 000 cells/well). Once confluent cells were stimulated for 48 h with IFN-γ (10 ng/mL). Gal-3 was measured in the supernatant (R&D systems, DGAL30).

RA SFMCs were also used for osteoclast differentiation.[41] Every 3 days culture medium was changed and supplemented with rh Receptor activator of nuclear factor kappa-B ligand (RANKL) (50 ng/mL, Abcam, ab157289) and rh Macrophage Colony-stimulating Factor (M-CSF) (25 ng/mL, Peprotech, 300–25). When media was changed the same treatment combinations of PD-1, PD-L1 and Gal-3 as described for HC PBMCs were administered. As a measure of osteoclast activity, levels of Tartrate-resistant acid phosphatase (TRAP) were measured in supernatants from day 21 using a commercially available kit (AK04, B-Bridge International, Inc.).

2.5 | Flow cytometry

PBMCs and SFMCs were stained for flow cytometry using anti-CD4 APC (clone: RPA-T4, BioLegend, 300 552), anti-CD8 AF700 (clone: RPA-T8, BD, 56–0088-41), anti-CD25 PerCP-Cy5.5 (clone: M-A251, BD, 560503), anti-PD-1 AF488 (clone: EH12.2H7, BioLegend, 329 936), anti-Gal-3 PE (clone: Gal397, BD, 126706), anti-IL-2 PECy7 (clone:

MQ1 17H12, BD, 560707) and nIR Live/Dead marker (Thermo Fisher, L34976), all at recommended concentrations. For intracellular staining the True-Nuclear™ Transcription Factor Buffer Set (Biolegend, 424 401) was used.

FLS were stained for flow cytometry using anti-CD90 BV605 (clone: 5E10, BioLegend, 328 128), anti-ICAM BV421 (clone: HA58, BD, 564077) and anti-PD-L1 PECy7 (clone: MIH3, BioLegend, 374 506) as well as intracellular: anti-Gal-3 PECF594 (clone: B2C10, BD, 565682).

Flow cytometric data acquisition was performed using the NovoCyte Quanteon® (ACEA Bioscience, San Diego, CA, USA) and flow cytometric analysis were performed in FlowJo™ 10.7.1. Gating was performed by including live, single cells. Additionally, gating was performed using fluorescence minus one (FMO) control (Figure S1, Figure S3+c).

2.6 | Immunofluorescence staining of synovial membranes

Formalin fixed, paraffin embedded sections of human RA synovial membranes were single-stained for either Gal-3 or PD-1. First, tissue sections were deparaffinated and rehydrated in Xylene and decreasing concentrations of ethanol, before demasking proteins in near-boiling Target Retrieval buffer (DAKO, S2369, pH 6). Tissue sections were blocked in 10% donkey serum and single-stained for PD-1 (20 μg/mL murine anti-human PD-1 antibody (clone: NAT105, Abcam, ab52587), secondary antibody: AF488 Donkey anti-mouse IgG (Jackson ImmunoResearch, 715-546-151) or Gal-3 (10 μg/mL rat anti-human Galectin-3 antibody (clone: M3/38, MABT51)), secondary antibody AF488 AffiniPure Donkey anti-rat IgG (Jackson ImmunoResearch, 712-546-153). For mounting and DAPI staining mounting media was applied (Invitrogen, P36941). Stained synovial membranes were examined using a Zeiss LSM800 confocal microscope. ImageJ was used to collect the signal from the z-stacks obtained on the microscope into one image with maximum signal of the section.

2.7 | Study approval

Human clinical studies were conducted in accordance with the Helsinki declaration. Informed written content was provided from all patients participating in the study. The INART biobank is approved by the ethical committee and the Danish Data Protection Agency (20121329). Plasma from anonymous HCs was obtained from the Danish blood bank.

2.8 | Statistics

Statistical analysis was performed using GraphPad Prism 9.1 (GraphPad Software).

Statistical analysis consisted of parametric tests (paired/unpaired t-tests) when data followed Gaussian distribution. If data did not meet Gaussian distribution criteria even after log-transformation, non-parametric tests were applied (Wilcoxon signed rank test (paired) or Mann–Whitney test (unpaired)). Graph whiskers represent standard deviation (SD). P-values ≤.05 were considered statistically significant (α = 0.05). When describing data following Gaussian distribution mean values ±95% confidence intervals were stated, while data not following Gaussian distribution were expressed as median (Interquartile range [IQR], Q1-Q3).

3 | RESULTS

3.1 | PD-1 and Gal-3 are highly expressed in the inflamed joint in RA

Levels of sPD-1 were significantly increased in RA SF compared to RA plasma. Further, RA plasma PD-1 levels were increased compared to HC plasma(Figure 1A). As for sPD-1, levels of Gal-3 were also increased in RA SF compared to RA plasma. Gal-3 plasma levels did not differ significantly between RA patients and HC (Figure 1B).

To further characterize the presence of PD-1 and Gal-3 in SF, we examined cellular expression on RA SFMCs, comparing to RA and HC PBMCs. Significantly more CD4+ T cells expressed PD-1+ in RA SFMCs compared to RA PBMCs and HC PBMCs (P <.01, Figure 1C). Upon stimulation, PD-1 expression increased significantly in all cell groups, with levels remaining highest in RA SFMCs after stimulation (Figure 1C). Expression of PD-1 among the CD4+ T cells did not differ between HC and RA PBMCs, neither before, nor after stimulation. As for PD-1, CD4+ T cells from unstimulated RA SFMCs expressed higher levels of Gal-3 compared to RA PBMCs. Upon stimulation, Gal-3 expression did not change significantly in any cell group. Expression of Gal-3 did not differ between HC and RA PBMCs (Figure 1D). When examining CD4+ T cells double positive for PD-1 and Gal-3, these were more abundant in RA SFMCs compared to RA PBMCs and HC (P <.05). Upon stimulation, the percentage of PD-1 +Gal-3+ expressing CD4+ T cells increased in all cell groups (Figure 1E). We further confirmed the presence of both PD-1 and Gal-3 in the RA synovium, by immunofluorescence staining of the synovial membrane. Both PD-1 and Gal-3 were expressed widely in the synovial membrane tissue sections; however, Gal-3 expression was more pronounced (Figure 1F).

—WILEY

FIGURE 1 Expression of soluble PD-1 and Gal-3 in SF and plasma and extracellular expression on PBMCs and SFMCs. A, PD-1 ELISA measuring levels of PD-1 in SF (n = 24) and plasma from RA patients (n = 9) and HC plasma (n = 7). B, Gal-3 ELISA measuring levels of soluble Gal-3 in SF (n = 25) and plasma (n = 7) from RA patients, and HC plasma samples (n = 5). C, Levels of PD-1+, D, Gal-3+ and E, PD-1 +Gal-3+ cells in CD4+ T cells from RA and HC PBMCs and RA SFMCs (n = 6 pr group) either unstimulated or stimulated with anti-CD3/anti-CD28. Stimulation upregulated PD-1 expression in RA and HC cells. Stimulation upregulated Gal-3 on RA PBMCs. F, Sections of synovial membrane from RA patients (n = 4). Left: Stained for Gal-3 visualized with AF488. Right: Stained for PD-1 also visualized with AF488. Nuclei are visualized with DAPI. Isotype controls presented below. *P*-values are indicated on graphs.
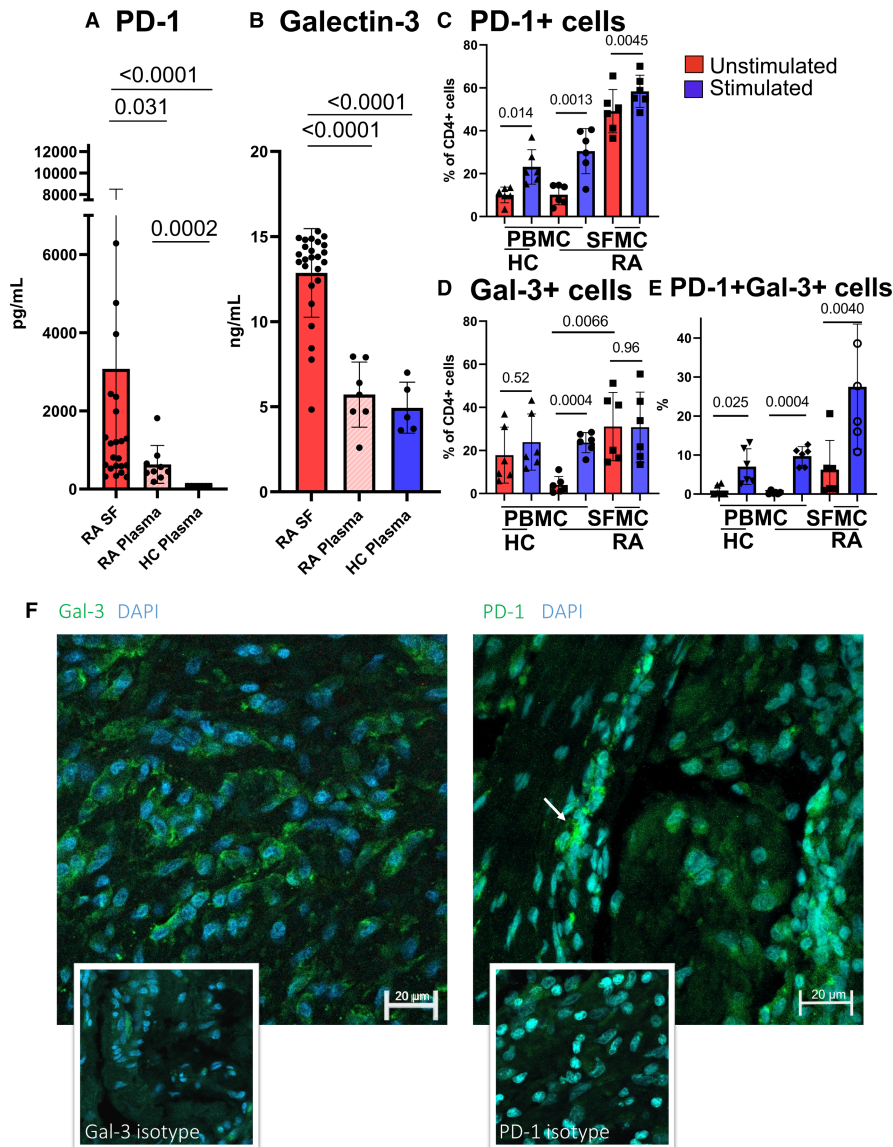
## 3.2 | Stimulating Fibroblast-Like Synoviocytes upregulates expression of PD-L1 and facilitates Gal-3 secretion

Next, we characterized the expression of PD-L1 and Gal-3 in inflammatory FLS defined as CD90+ICAM+. Stimulating FLS with either TNF-α or IFN-γ induced close to 100% ICAM-positive cells, supporting an activated state (Figure S3). Stimulation resulted in significantly higher percentage of PD-L1+ expressing FLS (Figure 2A), whereas stimulating cells with TNF-α induced a decreased percentage of Gal-3 expressing cells (Figure 2B). IFN-γ induced PD-L1 expression in nearly all cells, which was also demonstrated in the t-distributed stochastic neighbour embedding (t-SNE) plot (Figure 2E). The percentage of Gal-3+ cells was unaffected by IFN-γ stimulation (Figure 2B). Evaluating PD-L1+Gal-3+ inflammatory FLS, PD-L1 MFI was significantly increased by IFN-γ

stimulation and Gal-3 MFI was significantly decreased by both stimulations (Figure 2c+d). The decrease in intracellular Gal-3 levels upon stimulation was also visualized in the t-SNE plot (Figure 2E).

As intracellular Gal-3 decreased upon IFN-γ stimulation, we investigated if levels of secreted Gal-3 were affected by stimulation. Upon stimulation, Gal-3 in the supernatant increased significantly (Figure 2F). These results indicate how inflammatory FLS contribute to the higher extracellular levels of Gal-3 observed in synovial fluid from RA patients (Figure 1B).

3.3 | Gal-3 binds PD-1 and PD-L1

To establish the binding capacity between PD-1 and Gal-3 we used SPR. Increasing concentrations of rhGal-3 was subjected to the rhPD-1-coupled chip surface,
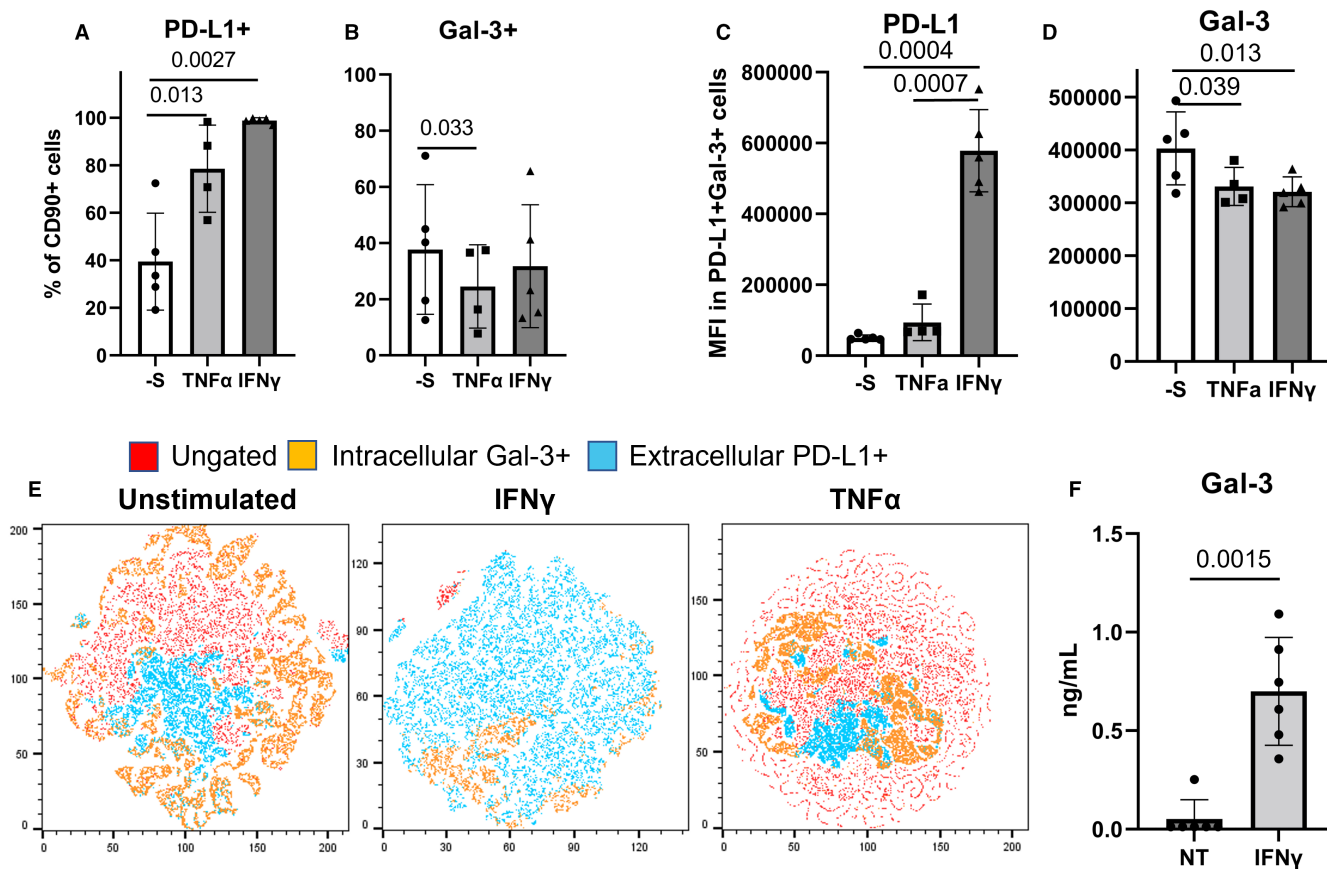
FIGURE 2 PD-L1 and Gal-3 expression levels on/in FLS. A, PD-L1 expression on CD90+ FLS unstimulated (-S) or treated with TNF-α or IFN-γ (n = 5). Stimulation significantly upregulated PD-L1. B, Gal-3 expression on CD90+ FLS unstimulated (-S) or treated with TNF-α or IFN-γ (n = 5). Levels of intracellular Gal-3 were significantly downregulated by TNF-α treatment. C, MFI of PD-L1 on PD-L1 + Gal-3+ FLS. IFN-γ stimulation significantly upregulates PD-L1 levels on PD-L1 + Gal-3+ FLS. D, MFI of Gal-3 in PD-L1 + Gal-3+ FLS. TNF-α and IFN-γ stimulation resulted in significant downregulation of intracellular levels of Gal-3 in PD-L1 + Gal-3+ cells. E, t-SNE plot of Unstimulated, IFN-γ- and TNF-α-treated FLS. IFN-γ stimulation significantly upregulates PD-L1 expression. F, Gal-3 ELISA on supernatants from FLS either unstimulated or stimulated with IFN-γ. Stimulation significantly increased levels of Gal-3 in FLS supernatants (n = 5).

which resulted in an increased mass on the chip surface measured in response units (RU), supporting binding between PD-1 and Gal-3 (Figure 3A). Quantitative evaluation of possible heterogenous binding was done using EVILFIT analysis,[42,43] which calculates the minimal distribution in binding kinetics for heterogeneous ligand interactions (Figure S2). The most abundant interaction between rhGal-3 and rhPD-1 had a K_D of 10^{-6}. For rhPD-L1 the K_D value was estimated to be approximately 10^{-5} (Figure S2). From the 2D-binding analysis we observed that the major population contributing to binding between Gal-3 and PD-1 had a slow dissociation rate and, therefore, would retain complex formation for an extended period of time ($k_{off} = 10^{-2,5}$ s^{-1}). The opposite was observed between Gal-3 and PD-L1 with the major contributor of binding having a dissociation rate of ($k_{off} = 10^{-0,5}$ s^{-1}). Still, both interactions showed multiple binding populations suggesting a that complex formation is not well-described by a simple 1:1 interaction. Furthermore, addition of lactose was able to inhibit the

interaction between rhGal-3 and rhPD-L1 in a dose dependent manner (Figure S2).

After demonstrating Gal-3 interaction with PD-1 and PD-L1 in vitro, we next examined whether rhGal-3 could bind sPD-1 from patient plasma and SF. The binding was confirmed using a combinatorial ELISA consisting of a Gal-3 protein coat and detecting bound PD-1 with an anti-PD-1 detection antibody. Furthermore, higher levels of sPD-1 binding to Gal-3 was seen in RA SF, compared to RA and healthy plasma, demonstrating that PD-1 from the inflamed environment still contained Gal-3 binding sites. (Figure 3B).

3.4 | Galectin-3 inhibits the anti-inflammatory function of PD-1 signalling in RA patients

We next investigated the potential effect of Gal-3 interacting with PD-1 upon T cell activation. We used intracellular
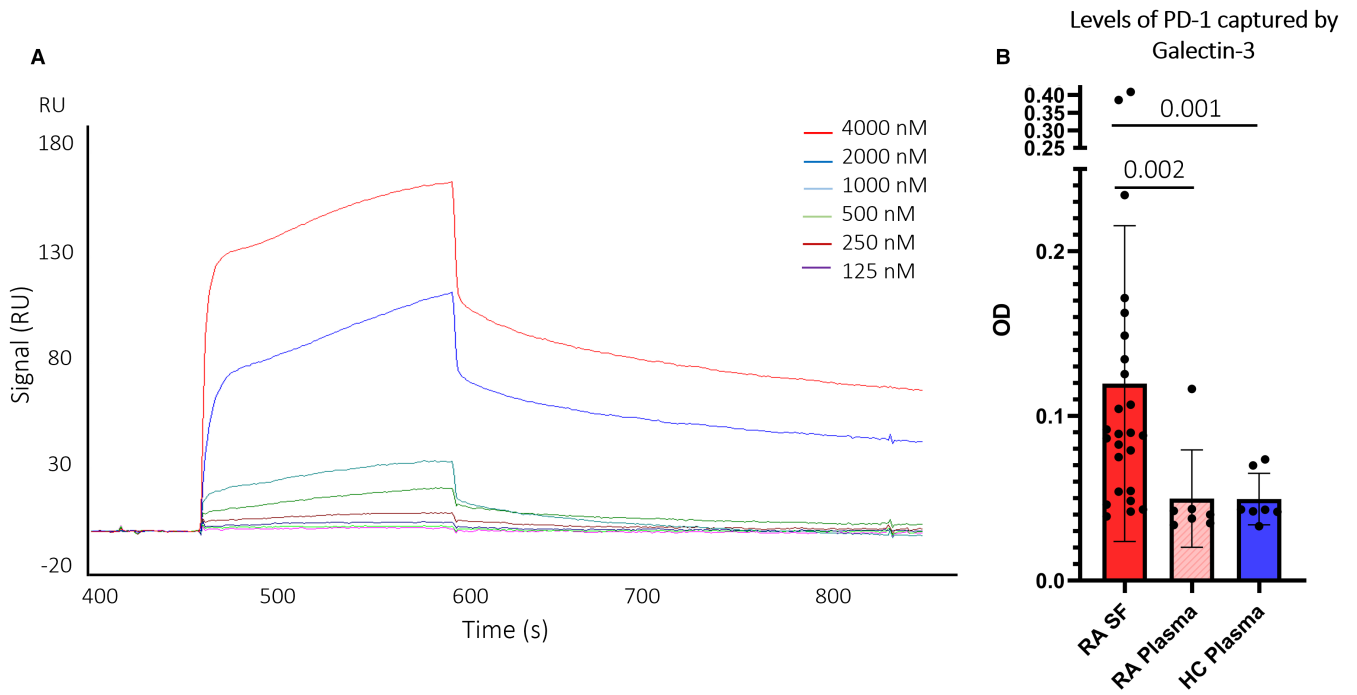
FIGURE 3 Binding of Gal-3 to PD-1 and PD-L1. A, Sensorgram of Gal-3 interaction with PD-1 coupled to the chip. Concentrations of Gal-3 in buffer ranges from 125-4000 nM. Binding visualized by rise in signal (response units, RU). Gal-3 is capable of binding PD-1. B, Combinatorial ELISA. Levels of soluble PD-1 in RA SF (n = 25) and plasma and HC plasma (n = 7, each) capable of binding immobilized rhGal-3. Levels expressed as blanked OD values. Significantly higher PD-1 levels in SF detected by rhGal-3 compared to RA plasma and HC plasma.
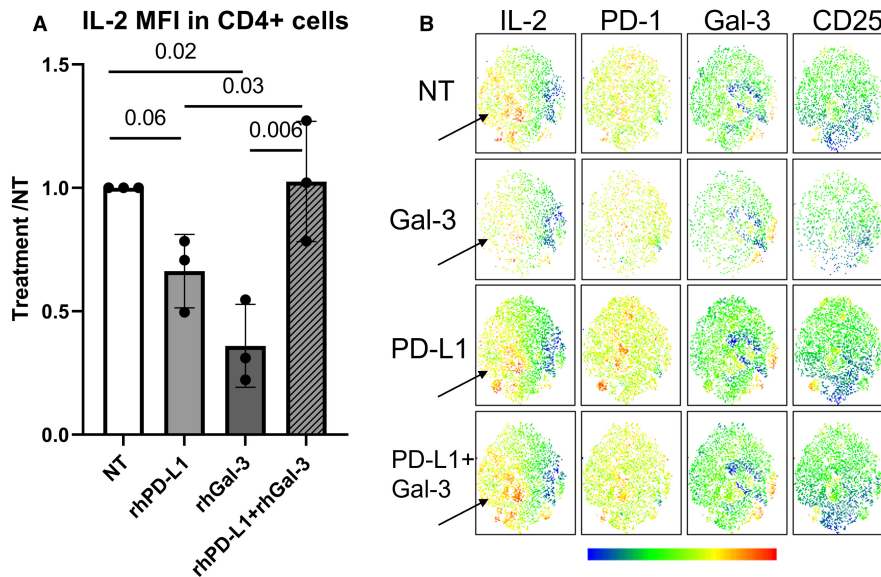
FIGURE 4 Functions of Gal-3 on cellular inflammation (IL-2) and the PD-1 signalling axis. A, Levels of IL-2 evaluated by MFI in CD4+ T cells treated with rhPD-L1, rhGal-3 or rhGal-3 combined with rhPD-L1. IL-2 MFI expressed as ratios calculated as: Treated / NT. rhPD-L1 slightly decreased intracellular IL-2 levels, while rhGal-3 significantly decreased intracellular IL-2 levels. B, t-SNE plot. Horizontal labels represent flow cytometric markers, whereas vertical labels represent cellular treatments before flow cytometry. IL-2 levels are downregulated in a specific cellular subset in CD4+ T cells treated with rhGal-3 or rhPD-L1 only, whereas the population reappears when cells are treated with both rhPD-L1 and rhGal-3 in combination (black arrows). N = 3.

IL-2 as a measure of T cell activation and reduced PD-1 signalling. Upon stimulation of CD4+ T cells, intracellular IL-2 levels decreased $33.75 \pm 12.14\%$ in the presence of rhPD-L1 compared to untreated CD4+ T cells. When adding rhGal-3 to the culture levels decreased significantly with $63.99 \pm 13.72\%$. However, combining rhGal-3 and rhPD-L1 reversed the effect and caused no decrease in IL-2 (Figure 4A). This effect was also visualized in the t-SNE plot, where levels of IL-2 in a specific subset decreases in cells treated with rhGal-3 or rhPD-L1 (Figure 4B). No effect was seen of rhPD-1 (Figure S3).

3.5 | Galectin-3 facilitates osteoclast formation while PD-L1 reduces osteoclast formation in RA patients

Joint and bone destruction are severe complications in RA and both PD-1 and Gal-3 are linked to the activity of osteoclasts. Hence, we investigated if Gal-3 interacting with the PD-1 pathway could influence osteoclast formation. Adding rhPD-L1 to RA SFMC osteoclast cultures slightly decreased TRAP activity after 21 days of culture, while rhGal-3 significantly increases TRAP activity. Combining rhGal-3 with rhPD-L1 in 1:1 stoichiometry demonstrated how rhPD-L1 plays a role in decreasing TRAP activity; however, rhPD-L1 was not able to significantly counteract the stimulatory effects of rhGal-3 in regard to osteoclast formation (Figure 5, Figure S4).

4 | DISCUSSION

Here, we report that Gal-3 binds to PD-1 and PD-L1 and that this interaction plays a role in inhibiting PD-1 signalling in RA Th cells and osteoclasts. Gal-3 and PD-1 were present in high levels in the inflamed RA joint, both as soluble forms and expressed by cells. Upon stimulation of T cells, PD-1 expression increased, whereas expression of Gal-3 remained unchanged. We also confirmed the interaction between PD-1 and Gal-3 in an inflammatory setting, capturing soluble PD-1 from the synovial fluid by Gal-3. These data are supportive of an interaction between PD-1 and Gal-3 in the inflamed synovium and suggest that the Gal-3 N-glycosylation binding sites on PD-1 are not changed in the highly inflamed microenvironment even though glycosylation is known to be modulated in this environment.[8]

Fibroblasts are central mediators of the inflammation in the RA joint,[5,6] and we suggest these cells, as a major source of extracellular Gal-3. This is supported by IFN-γ stimulation where intracellular Gal-3 decreased in concordance with increasing Gal-3 secretion. Decreased intracellular Gal-3 upon IFN-γ stimulation is previously reported.[44] Selectively targeting Gal-3 s CRD was reported to decrease FLS and osteoclast activity in RA,[27] and the present study adds a possible molecular explanation to the reduction in inflammation seen with a specific Gal-3 inhibitor.[45] Treatment with the Gal-3 inhibitor could potentially block the interaction between Gal-3 and PD-1/
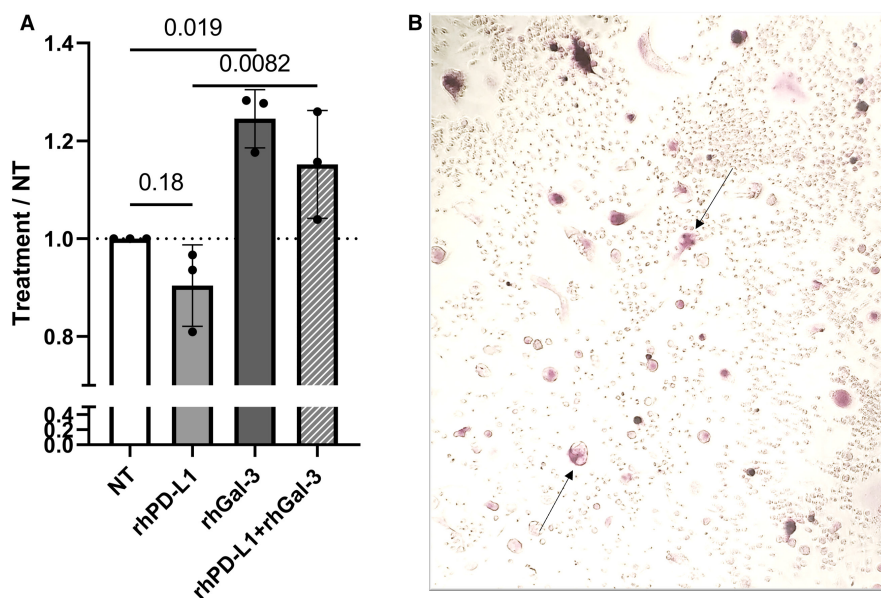
FIGURE 5 Osteoclast formation assay. A, TRAP assay on supernatants from SFMC osteoclast cultures after 21 days of stimulation with RANKL and M-CSF (NT) and indicated treatments. Formation presented as ratio, calculated: Treatment / NT. Cells treated with rhPD-L1 demonstrated a tendency towards decreased levels of TRAP activity. rhGal-3 significantly increased TRAP activity .rhPD-L1 and rhGal-3 in combination significantly increased TRAP activity compared to rhPD-L1 treatment only. RA SFMCs (n = 3). b) Image of osteoclasts generated from RA SFMCs. Black arrows marking examples of osteoclasts, identified as pink TRAP positive, multinucleated cells.

PD-L1 and hereby decrease both T cell and osteoclast activation.

We further highlighted the functional significance of Gal-3, influencing the PD-1 pathway. Adding Gal-3 to CD4 T cells cultured in the presence of rhPD-L1, significantly increased intracellular IL-2 levels, suggesting Gal-3 can reverse the inhibition mediated by the PD-1 pathway. The precise mechanism of this reversed inhibition remains to be elucidated, but a stimulatory role of Gal-3 has previously been described in IL-17 producing T cells from an RA mouse model.[28] Whether this effect is due to inhibition of immune checkpoint inhibitor receptors has not earlier been described. Another feature to consider is that the effect of Gal-3 seems to be dependent on the microenvironment, as well as type of disease and potentially also on the degree of ligand-induced multimerization of Gal-3. In RA, Gal-3 is associated with disease severity and inflammation, whereas the opposite effect has been observed in multiple types of cancer. In cancer, Gal-3 has been shown to have immunosuppressive effects, when present in the tumour microenvironment, thereby enabling the tumour to escape the immune system.[46,47] Multimerization can be induced in environments with high levels of Gal-3 ligands, for instance the high concentrations of PD-1 in RA synovium. This is supported by the slow dissociation rate for Gal-3 s binding to PD-1 demonstrated by SPR. Multimerization will result in high local levels of Gal-3, but also in increased functional affinity through increased avidity, which further facilitates the interaction between Gal-3 and PD-1 or PD-L1. The interaction could potentially hinder PD-1:PD-L1 interaction sterically in RA.

On the contrary, low sPD-1 levels have been observed in different types of cancer,[48] thus PD-1 is not available as a Gal-3 ligand to induce multimerization. Gal-3 could thus be in a monomeric form in certain types of cancer, explaining the different effects of Gal-3 in RA and cancer.

This corresponds with studies in breast cancer, where a germline mutation in Gal-3 abrogated formation of multimeric Gal-3, causing subjects to be more prone to develop cancer.[49,50] Therefore, monomeric Gal-3 might play a role in the immunosuppression seen in some cancers. In this study Gal-3 could also be in a monomeric form, when administered alone, since Gal-3 without ligand are known to behave as a monomer up to a concentration of $100\,\mu M$.[51] In contrast, multimeric Gal-3 dominates when Gal-3 is administered in combination with a ligand, for example PD-L1, resulting in a more pro-inflammatory effect of Gal-3, through inhibition of PD-1 signalling. Furthermore, K_D for Gal-3 s binding to PD-1 was estimated to be $1\,\mu M$, meaning that in the presence of high levels of Gal-3 ligand, here PD-1, the multimerization limit for Gal-3 is decreased by at least a factor 100. Thus

making, Gal-3 a local antagonist of PD-1 signalling in the synovium of RA patients, meaning Gal-3 is not desirable in RA. Elucidating whether the potential diversity in Gal-3′s function is dependent on its form is important knowledge when developing new treatment options in RA – as well as in different types of cancer.

A further addition to the diversity of Gal-3′s function is the many factors contributing to the complexity in RA synovium. One of these is Galectin-3 Binding Protein (G3BP). G3BP binds galectins such as Gal-3.[26,52] Since G3BP is also a highly glycosylated protein, elucidating the potential effect of G3BP on the PD-1:Gal-3 interaction is highly relevant, but beyond the scope of this study.

Finally, we provide evidence supporting that Gal-3 has a direct stimulatory effect on osteoclasts, thereby facilitating bone erosions. Gal-3 also play a role in preventing PD-L1 from decreasing osteoclast activity. These results support the hypothesis that PD-L1 and Gal-3 can interact and repel each other's effect. This effect of Gal-3 is supported by studies performed in mice.[28,30] The effect of PD-L1 is also supported by the literature demonstrating the importance of the PD-1 axis in maintaining bone homeostasis.[16]

5 | CONCLUSIONS

Collectively, this study suggests that Gal-3 binds to PD-1 and PD-L1. Presence of PD-1 and Gal-3 were demonstrated on mononuclear cells in blood and synovial fluid. The effects of Gal-3 differed between microenvironments, but when PD-L1 was present, Gal-3 had an inhibitory effect on PD-1 signalling. Furthermore, a sole pro-inflammatory and osteoclastogenic role of Gal-3 was observed in osteoclast cultures, both directly by osteoclast formation, but also though the PD-1 pathway. Thus, the main effect of Gal-3 on the PD-1 signalling axis are proposed to be inhibitory, meaning high Gal-3 levels in the complex synovial microenvironment are not desired in RA.

AUTHOR CONTRIBUTIONS

Kathrine Pedersen involved in formal analysis, investigation, writing the original draft editing and funding acquisition. Morten Aagaard Nielsen involved in conceptualization, methodology and original draft editing. Kristian Juul-Madsen involved in formal analysis and original draft editing. Malene Hvid involved in methodology and original draft editing. Bent Deleuran involved in conceptualization, supervision, project administration and original draft editing. Stinne Ravn Greisen involved in conceptualization, methodology, original draft editing and supervision.

CONFLICT OF INTEREST

Authors have no disclosures or competing interests.

DATA AVAILABILITY STATEMENT

Data available on request from the authors.

ORCID

Kathrine Pedersen https://orcid.org/0000-0002-3058-7960
Stinne Ravn Greisen https://orcid.org/0000-0003-2922-3307

REFERENCES

1. Bullock J, Rizvi SAA, Saleh AM, et al. Rheumatoid arthritis: a brief overview of the treatment. *Med Princ Pract*. 2019;27:501-507.

2. Heidari B. Rheumatoid arthritis: early diagnosis and treatment outcomes. *Casp J Intern Med*. 2011;2:161-170.

3. Li S, Yin H, Zhang K, et al. Effector T helper cell populations are elevated in the bone marrow of rheumatoid arthritis patients and correlate with disease severity. *Sci Rep*. 2017;7:1-11.

4. Sarkar S, Cooney LA, Fox DA. The role of T helper type 17 cells in inflammatory arthritis. *Clin Exp Immunol*. 2010;159:225-237.

5. Lee A, Qiao Y, Grigoriev G, et al. Tumor necrosis factor α induces sustained signaling and a prolonged and unremitting inflammatory response in rheumatoid arthritis synovial fibroblasts. *Arthritis Rheum*. 2013;65:928-938.

6. Kim KW, Cho ML, Lee SH, et al. Human rheumatoid synovial fibroblasts promote osteoclastogenic activity by activating RANKL via TLR-2 and TLR-4 activation. *Immunol Lett*. 2007;110:54-64.

7. Mohammadzadeh A. Co-inhibitory receptors, transcription factors and tolerance. *Int Immunopharmacol*. 2020;84:106572.

8. Sun L, Li CW, Chung EM, et al. Targeting glycosylated PD-1 induces potent anti-tumor immunity. *Cancer Res*. 2020;80:2298-2310.

9. Goods BA, Hernandez AL, Lowther DE, et al. Functional differences between PD-1+ and PD-1- CD4+ effector T cells in healthy donors and patients with glioblastoma multiforme. *PLoS One*. 2017;12:e0181538.

10. Arasanz H, Gato-Cañas M, Zuazo M, et al. PD1 signal transduction pathways in T cells. *Oncotarget*. 2017;8:51936-51945.

11. Han Y, Liu D, Li L. PD-1/PD-L1 pathway: current researches in cancer. *Am J Cancer Res*. 2020;10:727-742.

12. Greisen SR, Aspari M, Deleuran B. Co-inhibitory molecules – their role in health and autoimmunity; highlighted by immune related adverse events. *Front Immunol*. 2022;13:2782.

13. Raptopoulou AP, Bertsias G, Makrygiannakis D, et al. The programmed death 1/programmed death ligand 1 inhibitory pathway is up-regulated in rheumatoid synovium and regulates peripheral T cell responses in human and murine arthritis. *Arthritis Rheum*. 2010;62:1870-1880.

14. Guo Y, Walsh AM, Canavan M, et al. Immune checkpoint inhibitor PD-1 pathway is down-regulated in synovium at various stages of rheumatoid arthritis disease progression. *PLoS One*. 2018;13:e0192704.

15. Cutolo M, Sulli A, Paolino S, Pizzorni C. *CTLA-4 Blockade in the Treatment of Rheumatoid Arthritis: an Update.* Expert Review of Clinical Immunology; 2016. doi:10.1586/1744666X.2016.1133295

16. Greisen SR, Kragstrup TW, Thomsen JS, et al. Programmed death ligand 2 – a link between inflammation and bone loss in rheumatoid arthritis. *J Transl Autoimmun*. 2020;3:100028. doi:10.1016/j.jtauto.2019.100028

17. Greisen SR, Kragstrup TW, Thomsen JS, et al. The programmed Death-1 pathway counter-regulates inflammation-induced osteoclast activity in clinical and experimental settings. *Front Immunol*. 2022;0:673.

18. Chemin K, Gerstner C, Malmström V. Effector functions of CD4+ T cells at the site of local autoimmune inflammation-lessons from rheumatoid arthritis. *Front Immunol*. 2019;10:353.

19. Rao DA, Gurish MF, Marshall JL, et al. Pathologically expanded peripheral T helper cell subset drives B cells in rheumatoid arthritis *Nat*. 2017;5427639(542):110-114.

20. Yang R, Sun L, Li C, et al. Galectin-9 interacts with PD-1 and TIM-3 to regulate T cell death and is a target for cancer immunotherapy *Nat Commun*. 2021;121(12):1-17.

21. Barondes SH, Castronovo V, Cooper DNW, et al. Galectins: a family of animal β-galactoside-binding lectins. *Cell*. 1994;76:597-598. doi:10.1016/0092-8674(94)90498-7

22. Johannes L, Jacob R, Leffler H. Galectins at a glance. *J Cell Sci*. 2018;131:jcs208884. doi:10.1242/jcs.208884

23. Hu Y, Yéléhé-Okouma M, Ea HK, Jouzeau JY, Reboul P. Galectin-3: a key player in arthritis. *Joint Bone Spine*. 2017;84:15-20. doi:10.1016/j.jbspin.2016.02.029

24. Liu FT, Hsu DK, Zuberi RI, et al. Expression and function of galectin-3, a β-galactoside-binding lectin, in human monocytes and macrophages. *Am J Pathol*. 1995;147:1016-1028.

25. Mendez-Huergo SP, Hockl PF, Stupirski JC, et al. Clinical relevance of galectin-1 and galectin-3 in rheumatoid arthritis patients: differential regulation and correlation with disease activity. *Front Immunol*. 2019;10(9):3057.

26. Ohshima S, Kuchen S, Seemayer CA, et al. Galectin 3 and its binding protein in rheumatoid arthritis. *Arthritis Rheum*. 2003;48:2788-2795.

27. Nielsen M, Køster D, Greisen S, et al. Scandinavian Journal of Rheumatology ISSN: (Print) (Online) Journal homepage: https://www.tandfonline.com/loi/irhe20 Increased synovial galectin-3 induce inflammatory fibroblast activation and osteoclastogenesis in patients with rheumatoid arthritis. (2022). doi:10.1080/03009742.2021.1992860

28. Forsman H, Islander U, Andréasson E, et al. Galectin 3 aggravates joint inflammation and destruction in antigen-induced arthritis. *Arthritis Rheum*. 2011;63:445-454.

29. Wang CR, Shiau AL, Chen SY, et al. Intra-articular lentivirus-mediated delivery of galectin-3 shRNA and

galectin-1 gene ameliorates collagen-induced arthritis. *Gene Ther.* 2010;17:1225-1233.

30. Janelle-Montcalm A, Boileau C, Poirier F, et al. Extracellular localization of galectin-3 has a deleterious role in joint tissues. *Arthritis Res Ther.* 2007;9:R20.

31. Toegel S, Bieder D, André S, et al. Glycophenotyping of osteo-arthritic cartilage and chondrocytes by RT-qPCR, mass spectrometry, histochemistry with plant/human lectins and lectin localization with a glycoprotein. *Arthritis Res Ther.* 2013;15:R147.

32. Pivetta E, Scapolan M, Pecolo M, et al. MMP-13 stimulates osteoclast differentiation and activation in tumour breast bone metastases. *Breast Cancer Res.* 2011;13:R105.

33. Nakajima K, Kho DH, Yanagawa T, et al. Galectin-3 inhibits osteoblast differentiation through notch signaling. *Neoplasia (United States).* 2014;16:939-949.

34. Kragstrup TW, Vorup-Jensen T, Deleuran B, Hvid M. A simple set of validation steps identifies and removes false results in a sandwich enzymelinked immunosorbent assay caused by antianimal IgG antibodies in plasma from arthritis patients. *Springerplus.* 2013;2(1):263.

35. Salomonsson E, Carlsson MC, Osla V, et al. Mutational tuning of galectin-3 specificity and biological function. *J Biol Chem.* 2010;285:35079-35091. doi:10.1074/jbc.M109.098160

36. Jensen MR, Bajic G, Zhang X, et al. Structural basis for simvastatin competitive antagonism of complement receptor 3. *J Biol Chem.* 2016;291:16963-16976.

37. Juul-Madsen K, Qvist P, Bendtsen KL, et al. Size-selective phagocytic clearance of fibrillar α-synuclein through conformational activation of complement receptor 4. *J Immunol.* 2020;204:1345-1361.

38. Zhao H, Gorshkova II, Fu GL, Schuck P. A comparison of binding surfaces for SPR biosensing using an antibody-antigen system and affinity distribution analysis. *Methods.* 2013;59:328-335.

39. Stebulis JA, Rossetti RG, Atez FJ, Zurier RB. Fibroblast-like synovial cells derived from synovial fluid. *J Rheumatol.* 2005;32:301-306.

40. Køster D, Egedal JH, Lomholt S, et al. Phenotypic and functional characterization of synovial fluid-derived fibroblast-like synoviocytes in rheumatoid arthritis. *Sci Reports.* 2021;111(11):1.

41. Greisen SR, Einarsson HB, Hvid M, et al. Spontaneous generation of functional osteoclasts from synovial fluid mononuclear cells as a model of inflammatory osteoclastogenesis. *APMIS.* 2015;123:779-786.

42. Svitel J, Balbo A, Mariuzza RA, Gonzales NR, Schuck P. Combined affinity and rate constant distributions of ligand populations from experimental surface binding kinetics and equilibria. *Biophys J.* 2003;84:4062-4077.

43. Gorshkova II, Svitel J, Razjouyan F, Schuck P. Bayesian analysis of heterogeneity in the distribution of binding properties of immobilized surface sites. *Langmuir.* 2008;24:11577-11586.

44. Neidhart M, Zaucke F, von Knoch R, et al. Galectin-3 is induced in rheumatoid arthritis synovial fibroblasts after adhesion to cartilage oligomeric matrix protein. *Ann Rheum Dis.* 2005;64:419-424.

45. Vuong L, Kouverianou E, Rooney CM, et al. An orally active Galectin-3 antagonist inhibits lung adenocarcinoma growth and augments response to PD-L1 blockade. *Cancer Res.* 2019;79:1480-1492.

46. Iurisci I, Tinari N, Natoli C, et al. Concentrations of galectin-3 in the sera of normal controls and cancer patients. *Clin Cancer Res.* 2000;6:1389-1393.

47. Farhad M, Rolig AS, Redmond WL. The role of Galectin-3 in modulating tumor growth and immunosuppression within the tumor microenvironment. *OncoImmunology.* 2018;7:e1434467.

48. Ohkuma R, Ieguchi K, Watanabe M, et al. Increased plasma soluble pd-1 concentration correlates with disease progression in patients with cancer treated with anti-pd-1 antibodies. *Biomedicine.* 2021;9(12):1929.

49. Ruvolo PP. Galectin 3 as a guardian of the tumor microenvironment. *Biochimica et Biophysica Acta - Molecular Cell Research.* 2016;1863:427-437.

50. Balan V, Nangia-Makker P, Schwartz AG, et al. Racial disparity in breast cancer and functional germ line mutation in galectin-3 (rs4644): a pilot study. *Cancer Res.* 2008;68:10045-10050.

51. Lepur A, Salomonsson E, Nilsson UJ, Leffler H. Ligand induced galectin-3 protein self-association. *J Biol Chem.* 2012;287:21751-21756.

52. Lin TW, Chang HT, Chen CH, et al. Galectin-3 binding protein and galectin-1 interaction in breast cancer cell aggregation and metastasis. *J Am Chem Soc.* 2015;137:9685-9693.

SUPPORTING INFORMATION

Additional supporting information can be found online in the Supporting Information section at the end of this article.